Cardiovascular Magnetic Resonance in Cardiac Amyloidosis

Alicia Maria Maceira, MD; Jayshree Joshi, BSc; Sanjay Kumar Prasad, MD, MRCP; James Charles Moon, MB, MRCP; Enrica Perugini, MD; Idris Harding, BSc; Mary Noelle Sheppard, MD, FRCPath; Philip Alexander Poole-Wilson, MD, FRCP; Philip Nigel Hawkins, PhD, FRCP; Dudley John Pennell, MD, FRCP

Background—Cardiac amyloidosis can be diagnostically challenging. Cardiovascular magnetic resonance (CMR) can assess abnormal myocardial interstitium.

Methods and Results—Late gadolinium enhancement CMR was performed in 30 patients with cardiac amyloidosis. In 22 of these, myocardial gadolinium kinetics with T_1 mapping was compared with that in 16 hypertensive controls. One patient had CMR and autopsy only. Subendocardial T_1 in amyloid patients was shorter than in controls (at 4 minutes: 427±73 versus 579±75 ms; $P<0.01$), was shorter than subepicardium T_1 for the first 8 minutes ($P\leq0.01$), and was correlated with markers of increased myocardial amyloid load, as follows: left ventricular (LV) mass ($r=-0.51$, $P=0.013$); wall thickness ($r=-0.54$ to -0.63, $P<0.04$); interatrial septal thickness ($r=-0.52$, $P=0.001$); and diastolic function ($r=-0.42$, $P=0.025$). Global subendocardial late gadolinium enhancement was found in 20 amyloid patients (69%); these patients had greater LV mass (126±30 versus 93±25 g/m^2; $P=0.009$) than unenhanced patients. Histological quantification showed substantial interstitial expansion with amyloid (30.5%) but only minor fibrosis (1.3%). Amyloid was dominantly subendocardial (42%) compared with midwall (29%) and subepicardium (18%). There was 97% concordance in diagnosis of cardiac amyloid by combining the presence of late gadolinium enhancement and an optimized T_1 threshold (191 ms at 4 minutes) between myocardium and blood.

Conclusions—In cardiac amyloidosis, CMR shows a characteristic pattern of global subendocardial late enhancement coupled with abnormal myocardial and blood-pool gadolinium kinetics. The findings agree with the transmural histological distribution of amyloid protein and the cardiac amyloid load and may prove to have value in diagnosis and treatment follow-up. **(*Circulation*. 2005;111:195-202.)**

Key Words: amyloid ■ gadolinium ■ magnetic resonance imaging ■ heart diseases ■ cardiomyopathy

Cardiac involvement is frequent in systemic amyloidosis of immunoglobulin light chain (AL) and transthyretin (TTR) types and is a major determinant of treatment options and prognosis.[1] Cardiac involvement is the cause of death in approximately half of patients with AL amyloidosis,[2] is usually the sole manifestation of wild-type TTR amyloidosis (also known as senile cardiac amyloidosis), and is a major obstacle to therapeutic liver transplantation in many patients with variant TTR amyloidosis, the most common form of hereditary amyloidosis. Accumulation of these various proteins in the insoluble fibrillar amyloid conformation occurs principally in the myocardial interstitium,[3] leading to diastolic dysfunction progressing to restrictive cardiomyopathy.[4]

See p 122

The "gold standard" test for diagnosis of cardiac amyloidosis is myocardial biopsy,[5] but this is invasive and problematic. Thus, in practice, the diagnosis of cardiac amyloidosis is usually made by echocardiography, supported by a diagnostic noncardiac biopsy.[2,6] However, diagnosis by echocardiography has some limitations,[7] particularly if hypertrophy from other causes is present. Other noninvasive techniques also have limitations,[8] such as ECG[9] and scintigraphy with the use of radiolabeled serum amyloid P component (SAP).[10–12] Cardiovascular magnetic resonance (CMR) has not been evaluated in cardiac amyloidosis. Histologically, cardiac amyloidosis is characterized by interstitial expansion with amyloid protein[13,14] and associated endomyocardial fibrosis.[15] The late gadolinium enhancement CMR technique shows diagnostic abnormalities in conditions with expanded myocardial interstitial space, such as infarction,[16] hypertrophic cardiomyopathy,[17] and dilated cardiomyopathy.[18] We therefore hypothesized that CMR would show abnormalities in cardiac amyloidosis of diagnostic value.

Methods

Patients and Controls

We prospectively studied 29 newly presenting patients from the National Amyloidosis Centre of the United Kingdom between

Received April 30, 2004; revision received October 20, 2004; accepted October 25, 2004.

From the Cardiovascular Magnetic Resonance Unit (A.M.M., S.K.P., J.C.M., D.J.P.) and Department of Pathology (I.H., M.N.S.), Royal Brompton Hospital, London, UK; National Amyloidosis Centre, Royal Free Hospital, London, UK (J.J., P.N.H.); Istituto di Cardiologia, Hospital Sant Orsola, Bologna, Italy (E.P.); and Department of Cardiac Medicine, NHLI, Imperial College, London, UK (P.A.P.-W.).

Correspondence to Dr D.J. Pennell, CMR Unit, Royal Brompton Hospital, Sydney St, London SW3 6NP, UK. E-mail d.pennell@ic.ac.uk

Circulation **is available at http://www.circulationaha.org** **DOI: 10.1161/01.CIR.0000152819.97857.9D**

Baseline Characteristics of Patients and Controls

Characteristic	Amyloid Patients (n=29)	Hypertensive Controls (n=16)	P
Gender, male/female	15/14	9/7	0.77
Age, y	58±10	62±12	0.21
Body surface area, m^2	1.7±0.2	1.8±0.2	0.49
Weight, kg	64±12	67±8	0.32
Amyloid type			
Variant TTR	4	NA	NA
AL	25	NA	NA
LV end-diastolic volume, mL	100±27	140±36	<0.001
LV end-systolic volume, mL	40±19	52±23	0.07
LV stroke volume, mL	59±18	88±17	<0.001
LV ejection fraction, %	60±12	64±9	0.31
LV mass index, g/m^2	116±33	98±24	0.06
LV E/A wave velocity ratio	1.6±1.0	NA	NA
LV deceleration time, ms	170±40	NA	NA
Atrial septal thickness, mm	5.6±1.3	3.9±0.7	<0.001
Atrioventricular descent (septum), mm	7.3±3.8	12±4.1	0.001

Values are mean±SD. NA indicates not applicable.

August 2002 and April 2003. The baseline characteristics are shown in the Table. All patients had histological confirmation of amyloidosis by tissue biopsies (cardiac 2, noncardiac 27), with cardiac involvement diagnosed by echocardiographic criteria.[7,19] All had clinical assessment, ECG, echocardiography, ^{123}I-labeled SAP scintigraphy, and late gadolinium enhancement CMR. Myocardial gadolinium kinetics was studied in the last 22 amyloid patients and an additional 16 matched hypertensive controls who had no other cardiovascular abnormality from the clinical history and examination or by CMR (Table). One additional AL patient died suddenly 4 days after CMR only and underwent autopsy. Only patients with a contraindication to CMR were excluded. The ethics committee approved the study, and written, informed consent was obtained.

Amyloid Type

Amyloidosis was diagnosed with Congo red staining and demonstration of red-green birefringence under cross-polarized light. Immunohistochemical stains were performed on tissue sections with the use of commercial antisera against SAP, κ and λ immunoglobulin light chains, TTR, lysozyme, apolipoprotein AI, and fibrinogen.[20] In any cases of doubt, additional DNA analysis was performed. DNA was isolated from whole blood, and the genes were amplified and sequenced for TTR, apolipoprotein AI, fibrinogen A α chain, and lysozyme.

Echocardiography

Echocardiography was performed on a GE Vingmed System with the use of standard techniques.[21] The thickness of the left ventricular (LV) wall was determined from the M-mode at the level of the chordae. Pulsed Doppler of transmitral and pulmonary venous flow velocities was performed. At least 3 consecutive beats were measured and averaged for each measurement of the following: peak velocity of early (E) and late (A) filling waves; E/A ratio; and E-wave deceleration time. Cardiac involvement with amyloid was defined by the presence of morphological findings (eg, biatrial enlargement), a mean LV wall thickness >12 mm (in the absence of potential causes of hypertrophy),[7] and abnormal diastolic function from pulsed Doppler according to standard criteria,[7,19] with patients allocated into 3 dysfunctional filling pattern groups: slow relaxation, pseudonormal, or restrictive.[19]

SAP Scintigraphy

SAP was labeled with ^{123}I (100 μg SAP bearing 200 MBq) with the use of the *N*-bromosuccinimide method.[20] Thyroid uptake was blocked by oral potassium iodide for 2 days before and after isotope injection. Whole-body and abdominal imaging was performed after 24 hours (Elscint Super Helix). The extracardiac amyloid load was classified by an experienced observer as zero (no abnormal localization of tracer); small (uptake in at least one organ with normal blood-pool background signal intensity); moderate (abnormal uptake in at least one organ with reduction in the blood-pool background signal); or large (blood-pool background lost completely when the image gray scale was adjusted to encompass the target organ uptake).

Cardiovascular Magnetic Resonance

CMR was performed on a 1.5-T scanner (Siemens Sonata). For volumes, fast imaging with steady state precession (FISP) contiguous short-axis breath-hold cines were acquired from the atrioventricular ring to the apex (slice thickness 7 mm, repetition time/echo time 3.2/1.6 ms; temporal resolution 25 ms; retrospective gating; pixel size 2.4×1.5 mm; flip angle 60°; acquisition time 18 heartbeats). For late gadolinium enhancement imaging, a peripheral bolus injection (0.1 mmol/kg) of gadolinium-DTPA (Schering) was given, and images were acquired after 5 minutes with the use of a segmented inversion recovery sequence (segmentation was 13 to 25 lines, with triggering every 2 to 3 heartbeats). The DTPA is partitioned into the extracellular space, carrying the gadolinium as the contrast agent. In myocardium affected by increased extracellular space, gadolinium has a higher partition coefficient,[22] leading to significant signal enhancement, particularly if normal myocardium is nulled.[23] Late gadolinium enhancement CMR in the first 7 amyloid patients showed the unusual appearance of a dark blood pool and diminishing subendocardial enhancement over time, which suggested abnormal gadolinium-DTPA kinetics. Therefore, we developed a T_1 mapping method for the final 22 patients and compared them with controls. A magnetization prepared segmented FISP cine was developed with a 30-ms increment in inversion time for each frame. This was run every 2 minutes after the gadolinium bolus and was interleaved at each time point with late enhancement imaging.[23]

CMR Analysis

Ventricular volumes, function, and mass were analyzed with the use of semiautomated segmentation software (CMRtools, Cardiovascular Imaging Solutions). For analysis of the myocardial gadolinium kinetics, 2 doughnut-shaped regions of interest were drawn, incorporating the whole subendocardium (inner third of myocardium) and the whole subepicardium (outer third of myocardium) for each frame of the mapping series in a single midventricular slice; blood pool and background were also measured. An iterative computer model was written to obtain the T_1 from the null point of the curve relating the background-subtracted signal intensity and echo time. The model corrected for the influence on the T_1 recovery curve of the repeated time, FISP readout, FISP flip angle, segmentation, repetition time, myocardial T_1 and T_2, and delays between different components of the sequence.

Statistical Analysis

For the statistical analysis, SPSS software (SPS Inc) was used. All quantitative variables were found to conform to normality with the Kolmogorov-Smirnov test and are therefore presented as mean±SD. A 2-tailed Student *t* test was used to compare continuous variables, and the χ^2 or Fisher exact test was used for categorical variables. A repeated-measures mixed factorial design 3-way ANOVA was used to analyze the change in T_1, with time after gadolinium bolus injection, subjects, and subject group used as factors. Receiver operating characteristic (ROC) curves were plotted to determine the overall performance of different measurements for predicting cardiac amyloid. A probability value of <0.05 was considered statistically significant. Data are presented as mean±SD.

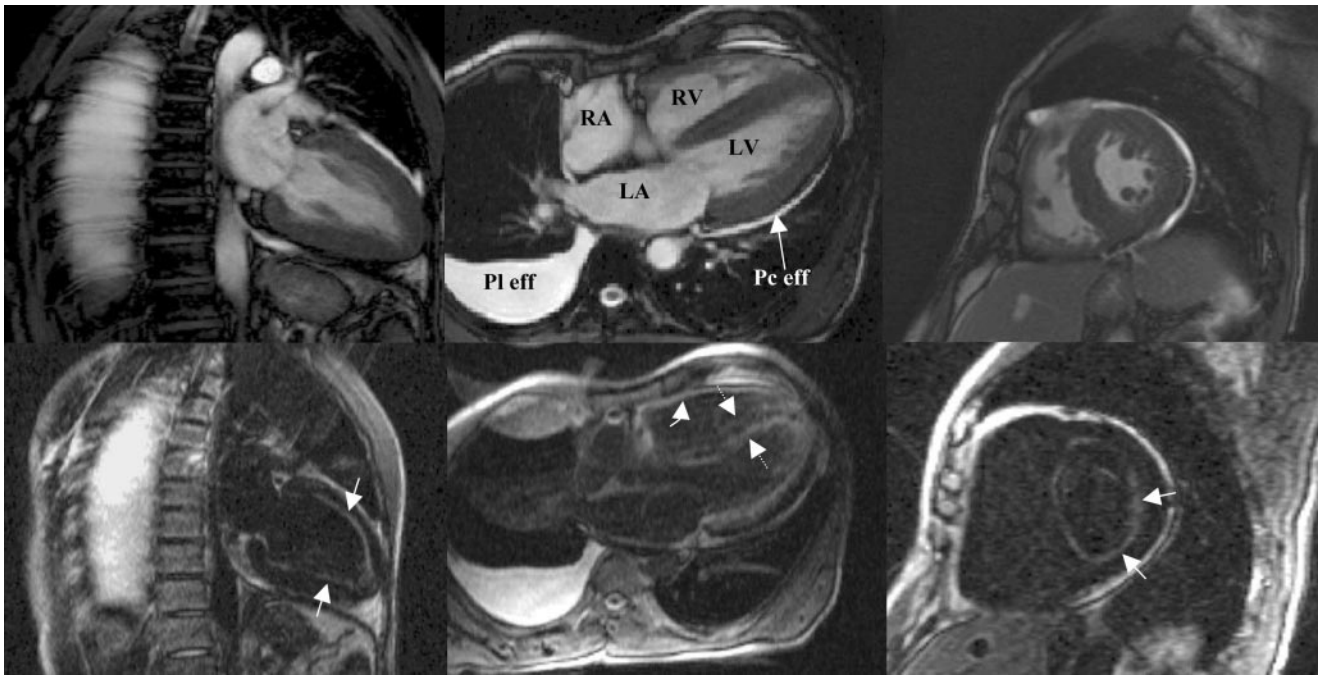

Figure 1. CMR in a patient with systemic AL amyloidosis. Top row shows diastolic frames from cines (vertical long axis, horizontal long axis, and short axis, respectively) showing a thickened LV and pleural effusions (Pl eff) and pericardial effusions (Pc eff) associated with heart failure. Bottom row shows late gadolinium enhancement images in the same planes. The CMR sequence forces myocardium remote from the pathology to be nulled (black) such that the abnormal region is enhanced. In cardiac amyloidosis, however, the region of greatest abnormality is enhanced as the entire myocardium is affected with amyloid infiltration, and the result is diffuse global subendocardial enhancement (straight arrows). The endocardium of the right ventricle (RV) is also heavily loaded with amyloid, and therefore the septum in the horizontal long axis view shows biventricular subendocardial enhancement with a dark midwall (zebra appearance; dotted arrows). The right ventricular free wall is also enhanced (curved arrow). Note that the blood pool is dark, which does not occur in other reported conditions, indicating abnormal gadolinium handling in these patients. LA indicates left atrium; RA, right atrium.

Results

Patients and Controls

The amyloid patients (n=29) and control subjects (n=16) were similar for age, gender, weight, and body surface area (Table). Relative to the normal range for LV mass index from our institution for FISP acquisitions (69±10 g/m^2), both amyloid patients (116±33 g/m^2; $P<0.001$) and hypertensive controls (98±24 g/m^2; $P<0.001$) had significant hypertrophy. The difference in LV mass index between amyloid patients and controls was not significant. The whole body amyloid load estimated by SAP scintigraphy was none/equivocal in 7 (24%), small in 11 (38%), moderate in 8 (28%), and large in 3 (10%). At the time of the CMR scan, 15 (52%) were in New York Heart Association (NYHA) heart failure class I, 11 (38%) in class II, 2 (7%) in class III, and 1 (3%) in class IV. In the amyloid patients, the end-diastolic volume and stroke volume were small compared with controls, and the atrioventricular descent was reduced, but the ejection fraction was similar. The atrial septal thickness was significantly greater in amyloid patients. Renal function (creatinine clearance) in the amyloid patients was 52±25 mL/min.

Late Gadolinium Enhancement

Myocardial late gadolinium enhancement was found in 20 patients (69%) and was subendocardial and global in all cases (Figure 1). No enhancement was found in the controls. The signal elevation from the enhanced regions was 186±68%. Contrast to noise ratio (CNR) between enhanced and nulled regions was 7±4. Enhancement was present in all TTR patients (100%) and 64% of AL patients ($P=0.20$). Comparisons were made between cardiac amyloid patients with or without myocardial enhancement. There was no significant difference in age, gender, or body surface area. In comparison with amyloid patients who showed no enhancement, the patients with myocardial enhancement had increased LV mass index (126±30 versus 93±25 g/m^2; $P=0.0094$), increased right ventricular mass index (44±8 versus 30±7 g/m^2; $P<0.001$), and lower LV ejection fraction (57±12 versus 67±7%; $P=0.029$). Of the patients with enhancement, 8 had impaired LV systolic function, in comparison with 0 patients with systolic dysfunction from the 9 patients without subendocardial enhancement ($P=0.029$). There were no significant differences between these groups in other hemodynamic parameters, diastolic function, NYHA class, or total body amyloid load.

Gadolinium Kinetics in Blood and Myocardium

Two minutes after injection, the blood T_1 was similar between amyloid patients and controls (287±60 versus 274±55 ms; $P=0.51$), but blood gadolinium clearance was significantly faster in amyloid patients, resulting in a higher blood T_1 over time (Figure 2A; $P<0.001$). Conversely, in the amyloid patients, the T_1 of subendocardium (367±61 versus 482±69 ms; $P<0.001$) and subepicardium (383±60 versus 492±69

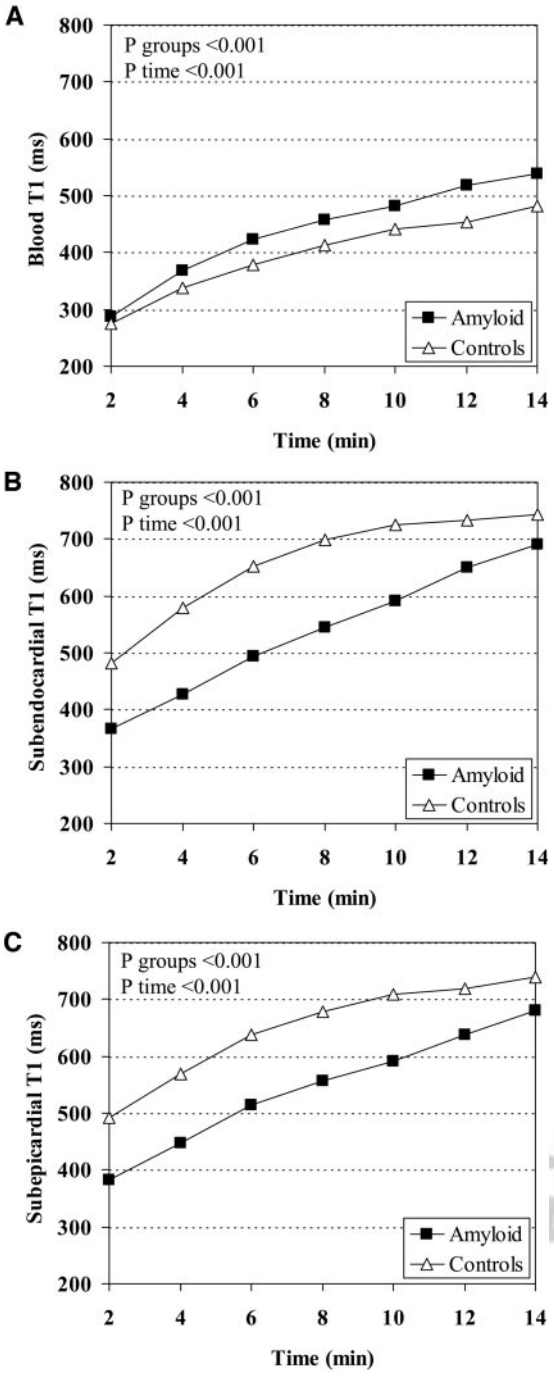

Figure 2. A, Blood T_1 is initially the same in patients with amyloidosis and controls, but faster gadolinium washout leads to a significantly higher T_1 in the amyloid patients. Subendocardial T_1 (B) and subepicardial T_1 (C) are initially significantly lower in the amyloidosis group than in controls, but this difference diminishes over time to near equivalence by 14 minutes.

ms; $P<0.001$) was significantly lower at baseline compared with controls (Figure 2B, 2C). These opposing effects resulted in the difference in T_1 between blood and myocardium being markedly diminished in the amyloid group (Figure 3). The T_1 of subendocardium in amyloid patients was significantly lower than subepicardium for 8 minutes after gadolinium injection, but after this no difference was seen (Figure 4A). This transmural difference was not present in the

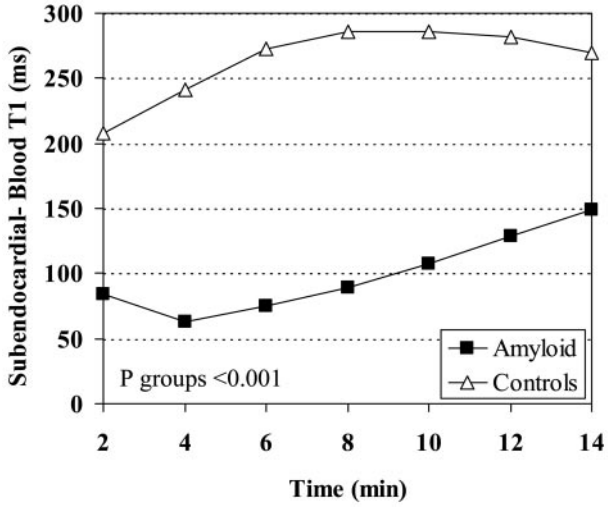

Figure 3. As a result of the abnormal blood and myocardium gadolinium kinetics, the difference between subendocardial T_1 and blood T_1 is substantially lower in the amyloidosis group than in controls.

controls (Figure 4B). Subendocardial T_1 over time was significantly lower in amyloid patients with late gadolinium enhancement than in those without enhancement ($P=0.004$), but for the subepicardium ($P=0.22$) and blood ($P=0.18$), this difference was not significant.

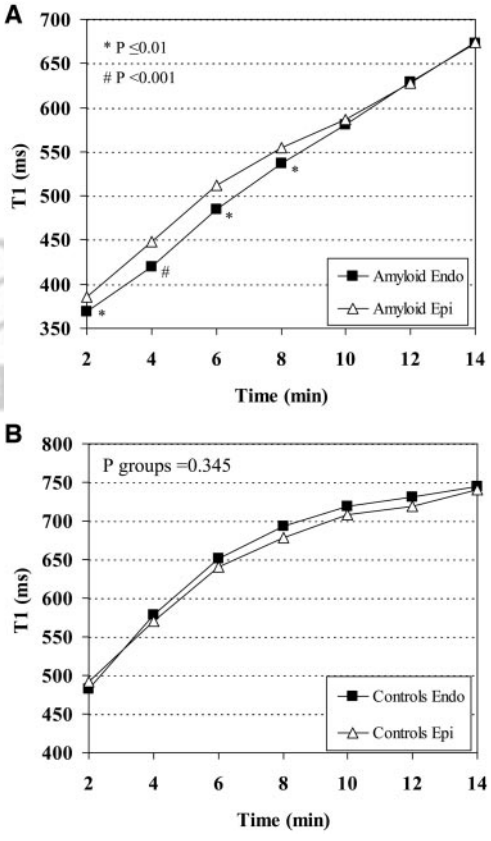

Figure 4. A, In amyloidosis, the subendocardial (Endo) T_1 is significantly lower than subepicardial (Epi) T_1 for 8 minutes after gadolinium injection, but the difference is lost after this time. B, In controls, no significant differences are present between endocardial and epicardial T_1.

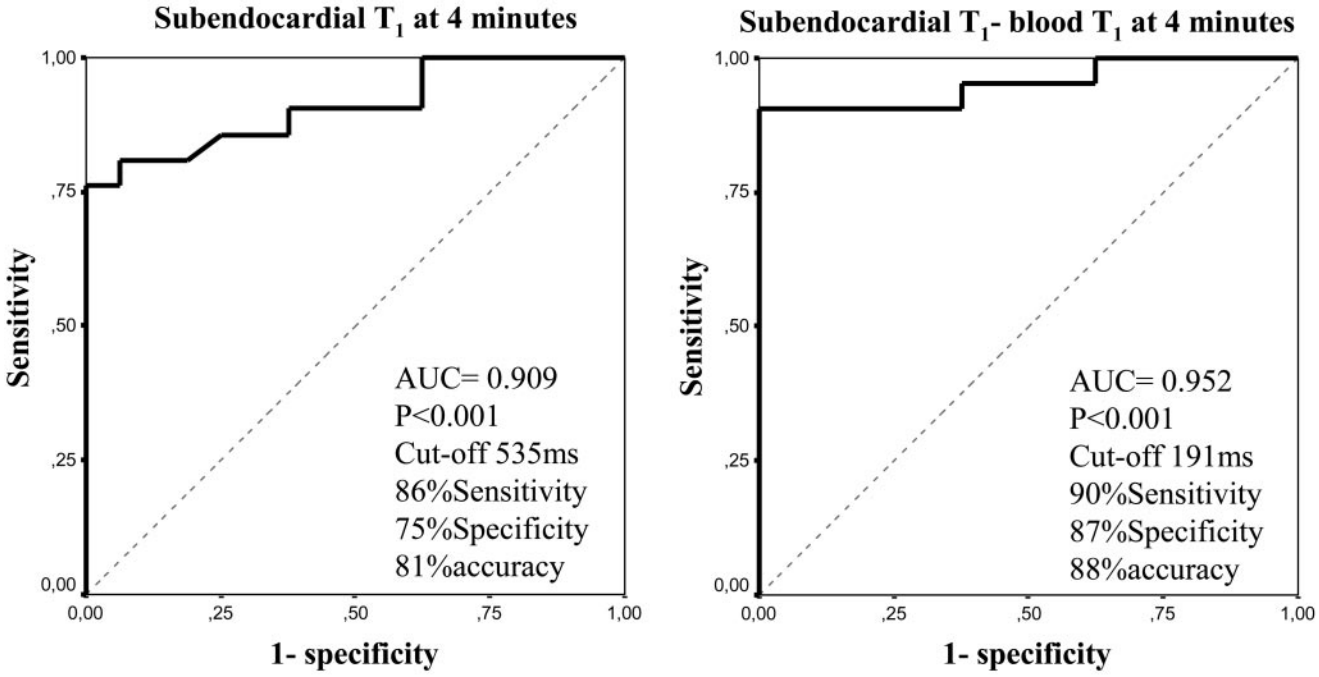

Figure 5. ROC curve for subendocardial T_1 (left) and the difference in subendocardial and blood T_1 (right) at 4 minutes after gadolinium injection for identifying cardiac amyloid.

Gadolinium Kinetics and Total Body Amyloid Load

The relation between blood gadolinium clearance, renal function, and total body amyloid load (as defined by SAP scintigraphy) was explored. Neither blood ($r=-0.12$, $P=0.62$) nor myocardial ($r=-0.15$, $P=0.53$) gadolinium clearance correlated with total body amyloid. Gadolinium clearance from the blood was faster in patients with impaired creatinine clearance ($r=-0.50$, $P=0.028$), but there was no relation between creatinine clearance and total body amyloid load ($r=-0.05$, $P=0.80$).

Myocardial T_1 and Diagnosis of Cardiac Amyloid

ROC analysis (Figure 5) showed that a subendocardial T_1 cutoff value of 535 ms at 4 minutes yielded an 81% accuracy for identifying cardiac amyloid (area under the curve [AUC]=0.909, $P<0.001$). This was surpassed, however, by the difference in T_1 between subendocardium and blood, which at a cutoff value of 191 ms at 4 minutes yielded an 88% accuracy (AUC=0.952, $P<0.001$). The accuracy of identification of cardiac amyloid was increased by combining the results from T_1 analysis and late gadolinium enhancement as diagnostic parameters, with 87% concordance for diagnosis using subendocardial T_1 and 97% concordance using the subendocardial-blood T_1 difference. Myocardial T_1 at 4 minutes was correlated with morphological markers of increased cardiac amyloid load, including LV mass index (subendocardial T_1 $r=-0.51$, $P=0.013$; subepicardial T_1 $r=-0.47$, $P=0.03$), ventricular thickness in all 4 walls (subendocardial T_1 $r=-0.54$ to -0.63, $P<0.04$; subepicardial T_1 $r=-0.54$ to -0.60, $P<0.03$), and interatrial septal thickness (subendocardial T_1 $r=-0.52$, $P=0.001$; subepicardial T_1 $r=-0.59$, $P<0.001$).

Myocardial T_1 and Cardiac Function

Reduced myocardial T_1 was correlated with smaller hearts and reduced systolic function: LV end-diastolic volume (subendocardial T_1 $r=0.53$, $P=0.001$; subepicardial T_1 $r=0.58$, $P<0.001$); LV stroke volume (subendocardial T_1 $r=0.51$, $P=0.002$; subepicardial T_1 $r=0.52$, $P=0.001$); LV septal longitudinal descent (subendocardial T_1 $r=0.60$, $P<0.001$; subepicardial T_1 $r=0.50$, $P=0.002$). There was no significant correlation between myocardial T_1 and ejection fraction, but there was a significant correlation between the subendocardial-blood T_1 difference and ejection fraction, but only at 2 minutes ($P=0.038$). There was a correlation between subendocardial T_1 and diastolic function at 6 minutes ($r=-0.42$, $P=0.025$), but the relation was stronger with the subendocardial-blood T_1 difference from 2 to 10 minutes after gadolinium ($r=0.44$ to 0.63, $P=0.02$ to <0.001). Myocardial T_1 was higher in the TTR than the AL group over time (subendocardium, $P=0.046$; subepicardium, $P=0.040$), but no other variable showed between group differences.

Autopsy Correlation

Autopsy from a patient with AL amyloidosis showed increased heart mass (705 g), increased LV thickness (20 mm), firm texture, ruddy coloration, and pale subendocardial areas. Congo red staining revealed interstitial nodular amyloid deposits, a fine perimysial network, and deposition in intramural coronary vessel walls without obstruction (Figure 6). Histological quantification showed substantial amyloid deposition (30.5% overall) with subendocardial predominance (42.4% versus midwall 29.2% versus subepicardium 17.6%) and little fibrosis (1.3% overall). The right ventricular subendocardium of the interventricular septum showed 47% amyloid deposition, and this was visualized as right ventric-

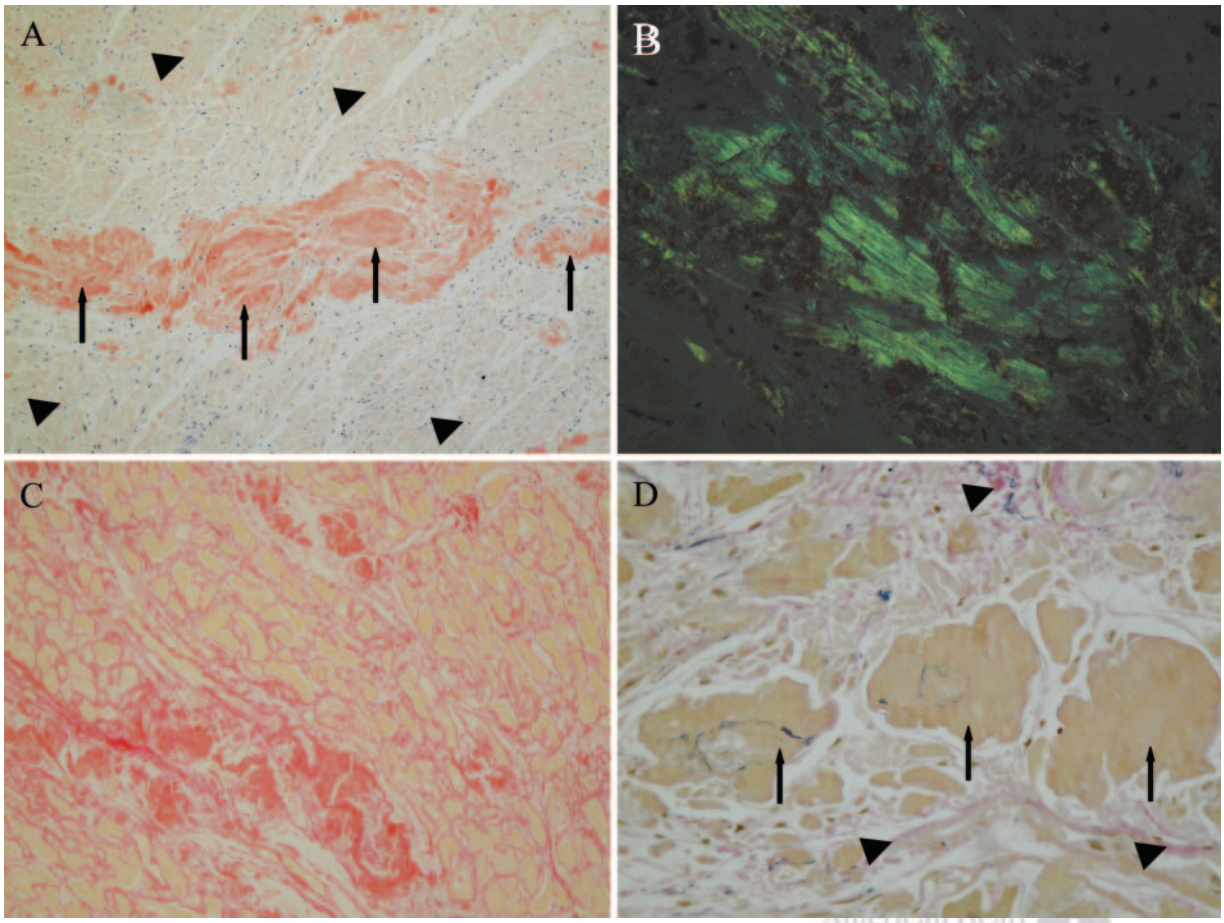

Figure 6. A, Congo red staining of section from postmortem heart. Substantial amyloid deposition is seen as red nodules (straight arrows), and there is fine interstitial infiltration around individual myocytes (arrowheads), confirmed by green birefringence under polarized light (B). C, Sirius red stains both amyloid and collagen, with myocytes staining yellow. Confirmation that the dominant component is amyloid comes from the elastin van Gieson stain (D), with amyloid showing as yellow (straight arrows) and collagen as dark pink (arrowheads). Note that there is only a small component of fibrosis.

ular endocardial enhancement, leading to a zebra pattern (Figure 1).

Discussion

In this study, CMR showed a characteristic pattern of abnormal myocardial and blood-pool gadolinium kinetics coupled with global subendocardial late enhancement in cardiac amyloidosis. The currently approved gadolinium chelates are all distributed in the extracellular space, and the enhancement depends on the time after injection and the CMR technique. During the first pass, myocardial perfusion is imaged with the use of multislice imaging with saturation recovery; early imaging with the use of inversion recovery is performed at 1 to 2 minutes to detect microvascular obstruction in acute myocardial infarction; and late imaging with inversion recovery is performed after at least 5 minutes to identify myocardial infarction and other causes of interstitial expansion. Late gadolinium enhancement occurs in areas of expanded extracellular space due to higher regional gadolinium concentration and slower distribution kinetics than in normal myocardium.[22,24] In chronic myocardial infarction[25] and hypertrophic cardiomyopathy,[26] the increased extracellular space results from fibrosis, and the same is probably true for dilated cardiomyopathy.[18] In other cardiomyopathies (Anderson-Fabry disease[27] and glycogen storage disease[28]), it is unclear whether the late gadolinium enhancement results from interstitial infiltration with the accumulated product from inherited deficient enzymatic pathways because histological confirmation is not yet available. Amyloidosis causes accumulation of an abnormal interstitial protein,[13,14] and we have demonstrated that this results in late gadolinium enhancement with a dominant subendocardial distribution that matches the transmural distribution of amyloid protein. The amount and transmural variation of amyloid protein (subendocardium 42.4%, subepicardium 17.6%) shows that this is the cause of the enhancement rather than the rather minor diffuse fibrosis (1.3%). This represents the first confirmation that nonfibrotic interstitial expansion can cause late gadolinium enhancement. The enhancement pattern in this study was subendocardial, diffuse, and global, which is different from that in infarction[16] and other cardiomyopathies[27,28] and the important differential diagnoses of hypertrophic cardiomyopathy[17] and hypertension (usually no significant enhancement).

Myocardium affected by amyloid had substantially lower T_1 at 4 minutes than controls. This appears to result from the myocardial amyloid deposition and is likely to represent a direct marker of the cardiac amyloid load. This is supported

by the correlation between myocardial T_1 and morphological measures of amyloid load such as LV mass. The gadolinium washout from blood and myocardium was faster than normal, probably because of gadolinium distribution into the total body amyloid load. The correlations of blood and myocardial gadolinium clearance to total amyloid load were not significant, however, which probably reflects the difficulties of assessing amyloid load with the use of SAP scintigraphy. Supportive of this concept was the significant relation between increased blood gadolinium clearance and impaired creatinine clearance; an interpretation of this finding is that the impaired renal function reflects an increased amyloid load. This is because impaired blood clearance of gadolinium-DTPA, as a small molecule, would not be expected until renal function was substantially impaired. The altered gadolinium kinetics was useful for diagnosis, with combined assessment of myocardial T_1 and global subendocardial late gadolinium enhancement yielding 87% diagnostic accuracy; this improved to 97% when the difference in T_1 between subendocardium and blood was used. Although other conditions could cause global subendocardial enhancement (such as endomyocardial fibrosis), distinguishing such conditions is readily accomplished clinically and by using the myocardial T_1 as a discriminating parameter.

The late gadolinium enhancement CMR was technically challenging. The dark blood pool resulted from similar myocardium and blood T_1 values because of high myocardial uptake and fast blood washout. The inversion time was shorter than normal and lengthened in larger incremental steps. The enhancement faded with equalization of T_1 between subendocardium and subepicardium at 8 minutes, and therefore imaging must be performed earlier than usual and completed quickly. The relative enhancement of the subendocardium was lower than previously reported; the percent signal elevation from enhanced myocardium in the amyloid patients was 186±68%, which is lower than in infarction (530±195%)[29] and hypertrophic cardiomyopathy (430±225%).[17] CNR was also lower between enhanced and nulled regions (7±4) than in infarction (19±3)[23] and hypertrophic cardiomyopathy (11.5±5.5).[17] This may result from a gradation in the density of the interstitial expansion, which is maximal in infarction in dense scar. In the autopsied heart, the amyloid was distributed with subendocardial predominance. This explains the subendocardial enhancement because myocardial nulling forces the subepicardium with relatively lower gadolinium uptake to appear darker, and it also explains the diffuse low enhancement because the increment in interstitial expansion between subendocardium and subepicardium is quite low compared with that between normal and infarcted myocardium.

Gadolinium CMR techniques may be used to assess and monitor the myocardial amyloid burden because no validated direct method exists, with poor correlation between echocardiography-derived burden, cardiac function, and prognosis.[15] CMR may also be used to assess the response to novel drugs in amyloidosis[30] and to elucidate paradoxical observations such as improved symptoms without reduction of LV wall thickness after chemotherapy and accelerated cardiomyopathy after orthotopic liver transplantation.[31] Sequential myocardial T_1 may be valuable for this because it directly reflects protein deposition as the primary pathological process.

Comparison With Other Techniques

The gold standard for diagnosis of cardiac amyloid is considered to be cardiac biopsy, although clinically significant amyloid can be missed with small biopsies because of heterogeneous deposition, and incidental wild-type TTR amyloid deposits occur in elderly patients.[32] ECG abnormality is a clue to cardiac disease,[33] but echocardiography is usually considered the technique of choice.[34] Antimyosin scintigraphy has high reported sensitivity for diagnosis of cardiac amyloid but modest specificity.[35] B-type natriuretic peptide[36] and cardiac troponins[37] may be elevated, but this occurs in many cardiac disorders, and the relative accuracy compared with echocardiography is unknown.

Study Limitations

Patient numbers were relatively small in this prospective study. The measurement technique for T_1 includes assumptions about the relaxivity of gadolinium-DTPA being the same in blood and myocardium. The diagnosis of cardiac amyloidosis did not routinely include endocardial biopsy, as is standard clinical practice in the UK National Amyloid Center. The total body amyloid loading in our patients by SAP scintigraphy was relatively low. However, SAP scintigraphy is typically equivocal or negative in patients with acquired or hereditary TTR amyloidosis, as it is in a modest proportion of patients with AL amyloid. A negative SAP scan does not exclude scattered amyloid deposits throughout the body or significant amyloid in certain organs (notably gut and peripheral nerves), but it excludes significant amyloid in certain viscera (notably liver, spleen, kidneys, bones). There is no correlation between the degree of cardiac involvement on echocardiography and whole body load at SAP scintigraphy.[38] We found no other significant correlations with total body amyloid load, and this reflects the limitations of this technique combined with study sample size. It might be possible to assess total body amyloid load from the blood gadolinium clearance, but this would vary with renal function, total body extracellular space, and cardiac output, all of which may be affected by amyloidosis, and we failed to identify significant relations with SAP scintigraphy. Our data do not compare the diagnostic value of CMR with echocardiography or other techniques, for which further comparative work is required. Likewise, any potential clinical role of these CMR techniques in populations with a lower prevalence of disease (patients with possible amyloidosis) is undefined. The reasons for only 64% of amyloid patients showing subendocardial enhancement may involve low cardiac amyloid burden relative to the sensitivity of late gadolinium enhancement CMR.

Conclusions

In cardiac amyloidosis, CMR shows high myocardial gadolinium concentrations early after injection, and global subendocardial late gadolinium enhancement is common. These findings have diagnostic value in this rare condition and may prove useful in the quantitative evaluation of the change in myocardial amyloid burden with new treatments.

Acknowledgments

This study was supported by CORDA and the British Heart Foundation. Research support was also received from Siemens Medical Solutions.

References

1. Kyle RA, Greipp PR, O'Fallon WM. Primary systemic amyloidosis: multivariate analysis for prognostic factors in 168 cases. *Blood*. 1986;68: 220–224.
2. Falk RH, Skinner M. The systemic amyloidoses: an overview. *Adv Intern Med*. 2000;45:107–137.
3. Arbustini E, Gavazzi A, Merlini G. Fibril-forming proteins: the amyloidosis: new hopes for a disease that cardiologists must know. *Ital Heart J*. 2002;3:590–597.
4. Nihoyannopoulos P. Amyloid heart disease. *Current Opin Cardiol*. 1987; 2:371–376.
5. Duston MA, Skinner M, Shirahama T, Cohen AS. Diagnosis of amyloidosis by abdominal fat aspiration: analysis of four years' experience. *Am J Med*. 1987;82:412–414.
6. Hamer JP, Janssen S, van Rijswijk MH, Lie KI. Amyloid cardiomyopathy in systemic non-hereditary amyloidosis: clinical, echocardiographic and electrocardiographic findings in 30 patients with AA and 24 patients with AL amyloidosis. *Eur Heart J*. 1992;13:623–627.
7. Klein AL, Hatle LK, Burstow DJ, Seward JB, Kyle RA, Bailey KR, Luscher TF, Gertz MA, Tajik AJ. Doppler characterization of left ventricular diastolic function in cardiac amyloidosis. *J Am Coll Cardiol*. 1989;13:1017–1026.
8. Dubrey SW, Cha K, Anderson J, Chamarthi B, Reisinger J, Skinner M, Falk RH. The clinical features of immunoglobulin light chain (AL) amyloidosis with heart involvement. *Q J Med*. 1998;91:141–157.
9. Reisinger J, Dubrey SW, Lavalley M, Skinner M, Falk RH. Electrophysiologic abnormalities in AL (primary) amyloidosis with cardiac involvement. *J Am Coll Cardiol*. 1997;30:1046–1051.
10. Hawkins PN, Myers MJ, Epenetos AA, Caspi D, Pepys MB. Specific localization and imaging of amyloid deposits in vivo using 123I-labeled serum amyloid P component. *J Exp Med*. 1988;167:903–913.
11. Hawkins PN, Pepys MB. Imaging amyloidosis with radiolabelled SAP. *Eur J Nucl Med*. 1995;22:595–599.
12. Hawkins PN, Richardson S, MacSweeney JE, King AD, Vigushin DM, Lavender JP, Pepys MB. Scintigraphic quantification and serial monitoring of human visceral amyloid deposits provide evidence for turnover and regression. *Q J Med*. 1993;86:365–374.
13. Laurent M, Toulet R, Ramee MP, Legrand D, Le Normand JP, Lelguen C. Light chain disease with terminal myocardiopathy. *Arch Mal Coeur Viss*. 1985;78:943–946.
14. Yazaki M, Tozuda T, Nakamura A, Higashikata T, Koyama J, Higuchi K, Harihara Y, Baba S, Kametani F, Ikeda S. Cardiac amyloid in patients with familial amyloid polyneuropathy consists of wild-type transthyretin. *Biochem Biophys Res Commun*. 2000;11:702–706.
15. Ishikawa Y, Ishii T, Masuda S, Asuwa N, Kiguchi H, Hirai S, Murayama A. Myocardial ischemia due to vascular systemic amyloidosis: a quantitative analysis of autopsy findings on stenosis of the intramural coronary arteries. *Pathol Int*. 1996;46:189–194.
16. Wu E, Judd RM, Vargas JD, Klocke FJ, Bonow RO, Kim RJ. Visualisation of presence, location and transmural extent of healed Q-wave and non-Q-wave myocardial infarction. *Lancet*. 2001;351:21–28.
17. Moon JCC, McKenna WJ, McCrohon JA, Elliott PM, Smith GC, Pennell DJ. Toward clinical risk assessment in hypertrophic cardiomyopathy with gadolinium cardiovascular magnetic resonance. *J Am Coll Cardiol*. 2003; 41:1561–1567.
18. McCrohon JA, Moon JC, Prasad SK, McKenna WJ, Lorenz CH, Coats AJ, Pennell DJ. Differentiation of heart failure related to dilated cardiomyopathy and coronary artery disease using gadolinium-enhanced cardiovascular magnetic resonance. *Circulation*. 2003;108:54–59.
19. Moyssakis I, Tripdskiadis F, Rallidis L, Hawkins P, Kyriakidis M, Nihoyannopoulos P. Echocardiographic features of primary, secondary and familial amyloidosis. *Eur J Clin Invest*. 1999;29:484–489.
20. Hawkins PN, Lavender JP, Pepys MB. Evaluation of systemic amyloidosis by scintigraphy with 123I-labeled serum amyloid P component. *N Engl J Med*. 1990;323:508–513.
21. Koyama J, Ray-Sequin PA, Falk RH. Longitudinal myocardial function assessed by tissue velocity, strain, and strain rate tissue Doppler echocardiography in patients with AL (primary) cardiac amyloidosis. *Circulation*. 2003;107:2446–2452.
22. Flacke SJ, Fischer SE, Lorenz CH. Measurement of the gadopentetate dimeglumine partition coefficient in human myocardium in vivo: normal distribution and elevation in acute and chronic infarction. *Radiology*. 2001;218:703–710.
23. Simonetti OP, Kim RJ, Fieno DS, Hillenbrand HB, Wu E, Bundy JM, Finn JP, Judd RM. An improved MR imaging technique for the visualization of myocardial infarction. *Radiology*. 2001;218:215–223.
24. Kim RJ, Chen EL, Lima JA, Judd RM. Myocardial Gd-DTPA kinetics determine MRI contrast enhancement and reflect the extent and severity of myocardial injury after acute reperfused infarction. *Circulation*. 1996; 94:3318–3326.
25. Weber KT, Sun Y, Campbell SE. Structural remodelling of the heart by fibrous tissue: role of circulating hormones and locally produced peptides. *Eur Heart J*. 1995;16(suppl N):12–18.
26. Moon JC, Reed E, Sheppard MA, Elkington AG, Ho SY, Burke M, Petrou M, Pennell DJ. The histological basis of late gadolinium enhancement cardiovascular magnetic resonance in hypertrophic cardiomyopathy. *J Am Coll Cardiol*. 2004;43:2260–2264.
27. Moon JC, Sachdev B, Elkington AG, McKenna WJ, Mehta A, Pennell DJ, Leed PJ, Elliott PM. Gadolinium enhanced cardiovascular magnetic resonance in Anderson-Fabry disease: evidence for a disease specific abnormality of the myocardial interstitium. *Eur Heart J*. 2003;24: 2151–2155.
28. Moon JCC, Mundy HR, Lee PJ, Mohiaddin RH, Pennell DJ. Myocardial fibrosis in glycogen storage disease type 3. *Circulation*. 2003;107:e47.
29. Kim RJ, Wu E, Rafael A, Chen EL, Parker MA, Simonetti O, Klocke FJ, Bonow RO, Judd RM. The use of contrast-enhanced magnetic resonance imaging to identify reversible myocardial dysfunction. *N Engl J Med*. 2000;16:1445–1453.
30. Pepys MB, Herbert J, Hutchinson WL, Tennent GA, Lachmann HJ, Gallimore JR, Lovat LB, Bartfai T, Alanine A, Hertel C, Hoffmann T, Jakob-Roetne R, Norcross RD, Kemp JA, Yamamura K, Suzuki M, Taylor GW, Murray S, Thompson D, Purvis A, Kolstoe S, Wood SP, Hawkins PN. Targeted pharmacological depletion of serum amyloid P component for treatment of human amyloidosis. *Nature*. 2002;417: 254–259.
31. Stangou AJ, Hawkins PN, Heaton ND, Rela M, Monaghan M, Nihoyannopoulos P, O'Grady J, Pepys MB, Williams R. Progressive cardiac amyloidosis following liver transplantation for familial amyloid polyneuropathy: implications for amyloid fibrillogenesis. *Transplantation*. 1998;66:229–233.
32. Sawabe M, Hamamatsu A, Ito T, Arai T, Ishikawa K, Chida K, Izumiyama N, Honma N, Takubo K, Nakazato M. Early pathogenesis of cardiac amyloid deposition in senile systemic amyloidosis: close relationship between amyloid deposits and the basement membranes of myocardial cells. *Virchows Arch*. 2003;442:252–257.
33. Rahman JE, Helou EF, Gelzer-Bell R, Thompson RE, Kuo C, Rodriguez ER, Hare JM, Baughman KL, Kasper EK. Non-invasive diagnosis of biopsy proven cardiac amyloidosis. *J Am Coll Cardiol*. 2004;43: 410–415.
34. Koyama J, Ray-Sequin PA, Falk RH. Longitudinal myocardial function assessed by tissue velocity, strain, and strain rate tissue Doppler echocardiography in patients with AL (primary) cardiac amyloidosis. *Circulation*. 2003;107:2446–2452.
35. Lekakis J, Dimopoulos M, Nanas J, Prassopoulos V, Agapitos N, Alexopoulos G, Palazis L, Kostamis P, Stamatelopoulos S, Moulopoulos S. Antimyosin scintigraphy for detection of cardiac amyloidosis. *Am J Cardiol*. 1997;80:963–965.
36. Palladini G, Campana C, Klersy C, Balduini A, Vadacca G, Perfetti V, Perlini S, Obici L, Ascari E, d'Eril GM, Moratti R, Merlini G. Serum N-terminal pro-brain natriuretic peptide is a sensitive marker of myocardial dysfunction in AL amyloidosis. *Circulation*. 2003;107: 2440–2445.
37. Dispenzieri A, Kyle RA, Gertz MA, Therneau TM, Miller WL, Chandrasekaran K, McConnell JP, Burritt MF, Jaffe AS. Survival in patients with primary systemic amyloidosis and raised serum cardiac troponins. *Lancet*. 2003;361: 1787–1789.
38. Clesham GJ, Vigushin DM, Hawkins PN, Pepys MB, Oakley CM, Nihoyannopoulos P. Echocardiographic assessment of cardiac involvement in systemic AL amyloidosis in relation to whole body amyloid load measured by serum amyloid P component (SAP) clearance. *Am J Cardiol*. 1997;80:1104–1108.